THE JOURNAL OF PHYSICAL CHEMISTRY B

Article

pubs.acs.org/JPCB

Thermodynamics of Micellization of Ionic Liquids C_6mimBr and Orientation Dynamics of Water for C_6mimBr−Water Mixtures: A Dielectric Spectroscopy Study

Xiaoqing Fan and Kongshuang Zhao*

College of Chemistry, Beijing Normal University, Beijing 100875, China

ABSTRACT: The aggregation behavior of C_6mimBr and its interaction with water at different concentrations and temperatures have been investigated by dielectric spectroscopy over frequency ranges from 500 MHz to 40 GHz. Dielectric determinations show that micellar aggregations form when the C_6mimBr concentration is higher than 0.85 M, and the size of micellar aggregations varies inversely to temperature. The thermodynamic quantities of the micellization at different temperatures, ΔG_m, ΔH_m, and ΔS_m were calculated, and it was found that the main driving forces of C_6mimBr aggregation were controlled by different thermodynamic quantities at different temperatures: the micelle formation process is controlled by an enthalpy effect at low temperature while it is entropically driven at high temperature. Two remarkable relaxations that originate from the orientation polarization of "bulk water" and "bound water" interacting with C_6mimBr were observed at about 8.2 and 15 GHz. The relaxation parameters obtained by fitting the dielectric spectra data were used to estimate the number of bound water per C_6mim^+ in the micellar core. The enthalpy and entropy closely linked to the relaxation processes of bound water and bulk water were calculated using the relaxation time according to Eyring equations. The average number of hydrogen bonds of a C_6mimBr−water system in different microenvironments was calculated, and the essence of cooperative orientation dynamics of water was described.

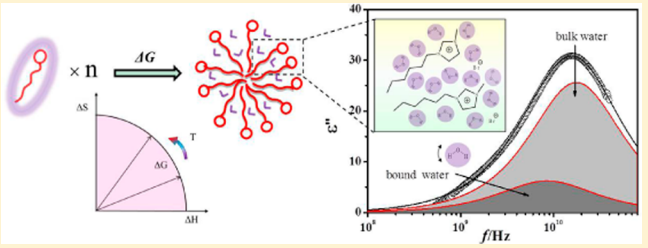

1. INTRODUCTION

Over the past decade, ionic liquids (ILs) have received much attention due to their unique properties, such as insignificant vapor pressures, high ion conductivity, high stability non-flammability, and wide electrochemical window, and have been widely applied in organic synthesis and catalysis, separation science, and life science.[1−3] On the basis of the design ability of ILs, one type of functional IL with a hydrophilic headgroup and hydrophobic tail analogous to traditional ionic surfactants was synthesized. Because of their inherent amphiphilic properties, they can be self-assembled into a variety of aggregates in aqueous solution and have received a great deal of attention in recent years.[4,5]

A large amount of research has focused on the interactions among amphiphilic molecules and with solvent because the physical process of amphiphilic self-assembly was governed by the balance between varieties of interactions.[6,7] The main effect on the aggregation behavior includes several factors: alkyl chain length, type of cations, and the nature of the counterions.[8,9] From the viewpoint of hydrophobic interaction, it is certain that the aggregation becomes more easy with an increase of the alkyl chain length of ILs. Recently, most studies have focused on the alkyl chain length from 8 to 16.[10,11] It is worth considering the length of the hydrocarbon chains in a given IL from well-defined aggregates. Some researchers[12,13] reported that oblate aggregates form at the critical micelle concentration (CMC) and the radius of aggregates increases with increasing C_6mimBr concentration. However, there exist different opinions and observations that C_6mim^{+}[14] has no CMC in an aqueous solution and C_8mim^{+}[15] does not micellize but forms an inhomogeneous solution of larger aggregates. The tendency of hydrophobic molecules to cluster in water is readily understood in terms of the dependence of hydrophobic solvation on solute size.[6] Hence, understanding the aggregation mechanism of ILs with critical alkyl chain length is fundamental and important for explaining the essential reasons for the aggregation processes of amphiphilic ILs and promoting their applications.

In addition to the effect of alkyl chain length, the interaction between amphiphilic ILs and solvent played a key role in the amphiphile assembly.[16] In the mixtures of ILs and water, the polar network of ILs was broken up by the added water molecules, which induced the microphase segregation between polar and nonpolar domains of ILs. Consequently, the nonpolar group (cation−cation) aggregation and water (water−anion−water) network were formed, indicating the existence of different organized nanostructures in ILs solution.[17,18] Meanwhile, some water molecules are confined within a small region of amphiphilic ILs because of the hydrogen bond interactions,[19,20] therefore their dynamical properties in these microenvironments are vastly different from those in bulk water. Moreover, the structural reorganization and

Received: July 2, 2014
Revised: October 28, 2014
Published: October 29, 2014

the peculiar thermodynamic signatures of water molecules surrounding hydrophobic molecule or hydrophilic surface are still being debated.[21] In short, the study of interaction between amphiphilic ILs and water and the resulting structural reorganization of water molecules that surround the ILs also help us understand the nature of their solution and aggregation behavior.

At present, the physicochemical property and aggregation structure of amphiphilic ILs have been studied by a variety of traditional physical techniques. For example, the surface tension measurements can provide CMC, surface tension at the CMC, adsorption efficiency, and effectiveness of surface tension reduction.[11,12] The degree of counterion dissociation and CMC in different temperatures can be measured by an electrical conductivity method based on which thermodynamics quantities of micelle formation process were calculated.[22−24] The information on micellar aggregation number (N), the morphology, and size of aggregation can be obtained by means of fluorescence quenching,[10,25] nuclear magnetic resonance (NMR),[13] and small-angle neutron scattering methods (SANS).[12,26] However, there are few reports in the research about microstructure changes before and after micelle formation such as the number of bound water per ILs, the change in the microenvironment surrounding ILs, and the structural reorganization of water molecules. This exactly reflects the nature of the solubility and aggregation behavior of amphiphilic ILs.

It is generally known that dielectric relaxation spectroscopy (DRS), owing to its sensibility to the polarization process, has been extensively used to provide insight into the structural and dynamics properties of all kinds of liquid systems at molecular and macroscopic levels.[27−29] Shikata et al.[30] discussed the number of hydrated water molecules per poly(*N*-isopropylacrylamide) (P(NIPAm)) monomer unit by analyzing the dielectric parameters of aqueous P(NIPAm) solutions, relaxation time, and dielectric increment. They suggested that hydrogen bond bridges between all of the water molecules involved in hydration were produced. Buchner et al.[31] presented a detailed DRS study on the aqueous solutions of the two simplest carboxylate ions, sodium formate and sodium acetate. They found that very few (<2 per anion) water molecules were irrotationally bound, and water molecules with reduced dynamics result from the relatively strong hydrophilic interaction of water with the $-COO^-$ moiety.

In the present paper, the dielectric spectra of a series of mixtures composed of C_6mimBr with short alkyl chain and water have been investigated in a wide temperature range. By analyzing the direct current (dc) conductivity of C_6mimBr aqueous solution in different temperatures, the main driving forces of C_6mimBr aggregation are fully discussed. On the basis of the relaxation parameters of two dielectric relaxations, the numbers of bound water per C_6mim^+ in the micellar core were obtained. Furthermore, orientation dynamics of water molecules in different microenvironments were explored. It is expected that the results obtained in the present work can contribute more information to the fundamental understanding of amphiphilic ILs and their applications.

2. MATERIALS AND METHODS

2.1. Materials. The ILs C_6mimBr (purity >99%, 4.7 mol/L) was purchased from Shanghai Cheng Jie Chemical Co. Ltd., China. The residual chloride in this IL was less than 800 ppm, and the water content was less than 1000 ppm. The molecular structure of C_6mimBr is depicted in Scheme 1. A series of C_6mimBr concentrations were prepared from 0.4 to 2.11 M (from 0.83% to 6.46% in the mole fraction unit). Doubly distilled water was used throughout all of the experiments.

Scheme 1. Chemical Structure and Atom Numbering of Surface-Active Imidazolium ILs C_6mimBr

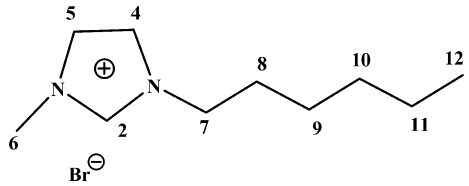

2.2. Dielectric Measurements. The dielectric spectra were measured with an Agilent E8362B PNA series network analyzer (Agilent Technologies, made in America) equipped with an Agilent 85070E open-ended coaxial probe (Agilent Technologies, made in America), which covers the frequency ranges from 500 MHz to 40 GHz. All measurements were carried out in the temperature ranges from 288.2 to 323.2 K (±0.2 K). The permittivity ε and total dielectric loss ε'' were automatically calculated as functions of frequency by the built-in software of this measuring system, which was calibrated in accordance with the procedures recommended by the manufacturers. The dielectric measurement in each temperature was completed in seconds.

2.3. Determination of Dielectric Parameters. The dielectric relaxation parameters were obtained by fitting the following equation to the experimental dielectric data

$$\varepsilon^* = \varepsilon(\omega) - j\varepsilon''(\omega) = \varepsilon_h + \sum_i \frac{\Delta\varepsilon_i}{1 + (j\omega\tau_i)^{\beta_i}} \quad (1)$$

where, ε_h is the high frequency limit of permittivity, $\Delta\varepsilon_i$ is the dielectric increment (or relaxation intensity) of the relaxation mode i, $j^2 = -1$, $\tau_i = 1/(2\pi f_i)$ (f_i is the characteristic relaxation frequency) denotes the relaxation time of the relaxation mode i, and β_i ($0 < \beta_i \leq 1$) is the parameter related to the distribution of relaxation time.

3. RESULTS AND DISCUSSION

3.1. Microwave Dielectric Behavior for the Binary System C_6mimBr−Water. Figure 1 shows the dielectric spectra (a) and dielectric loss spectra (b) (which are the real and imaginary parts of complex permittivity ε^* in eq 1, respectively) for C_6mimBr aqueous solution in the concentration range of 0.4−2.11 M. Remarkably, both permittivity and dielectric loss spectra show distinct dielectric relaxation at the frequency ranges from 500 MHz to 40 GHz. The dielectric increment and relaxation frequency decrease as the C_6mimBr concentration increases as shown by arrows. The steep rise in dielectric loss with the decrease of frequency below about 5 GHz (circled by a dashed ring in Figure 1b) originates from higher dc conductivity κ_l. All of the relaxation parameters that appear in eq 1 are obtained by fitting these data in Figure 1a with eq 1 and are summarized in Table 3.

For the aqueous system with higher conductivity, eq 1 is generally shown as[32]

$$\varepsilon^*(\omega) = \varepsilon(\omega) - j\frac{\kappa(\omega)}{\varepsilon_0\omega} = \varepsilon(\omega) - j\varepsilon''(\omega) - j\frac{\kappa_l}{\varepsilon_0\omega} \quad (2)$$

dx.doi.org/10.1021/jp506589f | J. Phys. Chem. B 2014, 118, 13729−13736

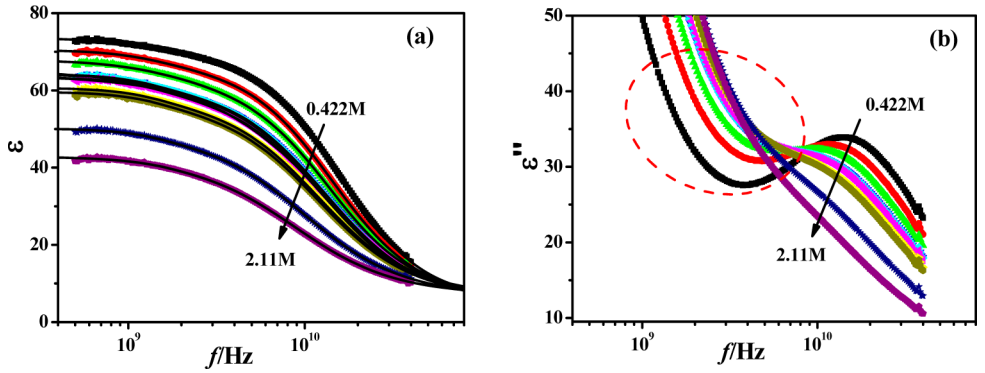

Figure 1. Frequency dependency of dielectric spectra (a) and dielectric loss spectra (b) of C_6mimBr aqueous solution of different concentrations. The black lines represent the best-fit curves.

That is to say, the real dielectric loss ε''_{rel} is obtained by subtracting the dc conductivity contribution ε''_{dc} from the total dielectric loss $\varepsilon''(\omega) = \kappa(\omega)/\varepsilon_0\omega$. The dc conductivity contribution can be expressed as[33]

$$\varepsilon''_{dc} = \kappa_l/\varepsilon_0\omega \quad (3)$$

Here, κ_l was obtained by fitting the raw dielectric loss with eq 3 and is the scaling dependence of total dielectric loss with a slope −1 on ω. All of the dielectric spectra data shown in Figure 1 were recalculated, and the corrected dielectric loss spectra were obtained according to the above method. Figure 2 shows an example of dielectric loss spectra after subtraction of the dc conductivity contribution for 0.633 M C_6mimBr solution.

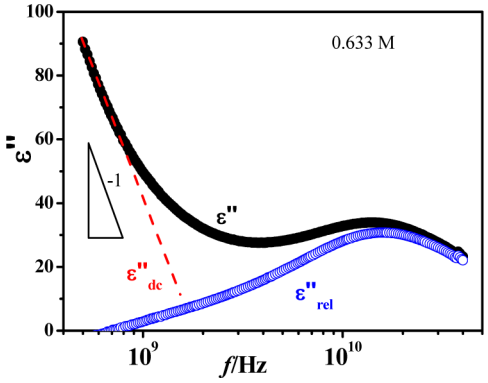

Figure 2. Dielectric loss spectra of 0.633 M C_6mimBr solution. Black solid circles represent raw experimental data, the red line indicates the dc conductivity contribution, and the blue hollow circles represent experimental data after subtracting dc conductivity contribution.

3.2. Micellization of C_6mimBr in Water. The values of κ_l for C_6mimBr solution, which are extracted from imaginary parts of complex permittivity ε^*, are plotted as a function of concentration in Figure 3. With the gradual increase of concentration, an abrupt change in the conductivity−concentration curve can be observed at a concentration of about 0.8 M. That is, micellar aggregations form when the C_6mimBr concentration is larger than 0.8 M, which is taken as the CMC of C_6mimBr. In the low concentration domain, the polar network of C_6mimBr is entirely broken up by the intruding water, so κ linearly increases with the concentration due to the growing number of C_6mim^+ and Br^- ions. However, when the concentration is larger than 0.8 M, the increase was

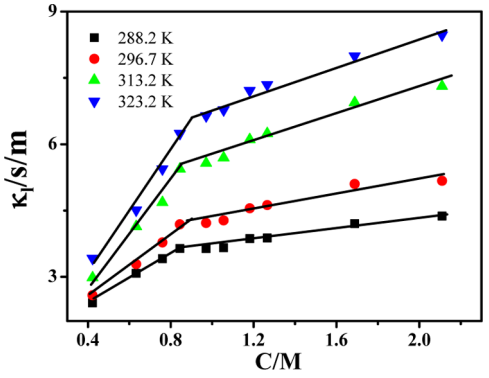

Figure 3. Plots of dc conductivity, κ_l, against C_6mimBr concentration, C, at different temperatures.

inhibited for the formation of the nonpolar group aggregation. This is because the partial anions Br^- are confined to the aggregation surface.

To confirm the micelle formation, the CMC and the slopes were obtained by fitting the $\kappa-C$ data in Figure 3 with eq 4[34] and are summarized in Table 1.

$$K = S_1C + p(S_2 - S_1)\ln\left(\frac{1 + \exp[(C - CMC)/p]}{1 + \exp(-CMC/p)}\right) \quad (4)$$

Here, S_1 and S_2 are the gradients of the $\kappa-C$ curve below and above the CMC, respectively, p is the width of the transition, C is the C_6mimBr concentration, and CMC represents the central point of the transition. The values of CMC are in good agreement with those obtained by surface tension,[12] fluorescent probe technique,[22] and NMR[13] as shown in Table 1.

In Table 1, the degree of counterion dissociation, α, was obtained from the ratio of the slopes above and below the break point of CMC. $1 - \alpha$ is defined as the degree of counterion binding and denoted by γ, which indicates the ability of the counterions in C_6mimBr binding to micellar surface. Table 1 shows a larger value of γ (0.74−0.84), which indicates the larger volume of the C_6mimBr micelle. This is because the electrostatic attraction between C_6mim^+ and Br^- is stronger than the self-repulsion between C_6mim^+ groups; consequently, the binding capacity of Br^- is enhanced. As a result, N of the micelle increases and the volume also becomes larger.[35,36] In addition, γ decreases with the increase in temperature, which suggests that C_6mimBr forms smaller micelle aggregation in

dx.doi.org/10.1021/jp506589f | J. Phys. Chem. B 2014, 118, 13729−13736

Table 1. Parameters Obtained by Fitting eq 4 to Conductivity Data

T (K)	CMC (M)	S_1 (S cm^2 mol^{-1})	S_2 (S cm^2 mol^{-1})	α (= S_2/S_1)	CMC[a] (M)
288.2	0.819	3.157	0.516	0.163	
296.7	0.845	3.768	0.873	0.194	0.8,[12] 0.88,[22] 0.79[13]
313.2	0.851	5.968	1.502	0.247	
323.2	0.854	6.627	1.759	0.265	

[a]Literature values.

higher temperature, consistent with the results from dynamic light scattering[37] and SANS.[38]

Further, the fundamental parameter of micellar aggregation, N, was estimated by the following equation, $N = (4\pi l^3/3V)$ (where V is the effective hydrophobic chain volume and l is the alkyl chain length in the micellar core, whose values are given by Tanford's formulas[39]). N for C_6mimBr is determined to be 13, which is also comparable to other results for C_6mimBr.[13] Compared with N of C_8mimBr, C_{10}mimBr, and C_{12}mimBr (N = 21, 38, and 45, respectively),[22] it can be see that N increases with an incremental increase of the alkyl chain length by one methylene group.

3.3. Thermodynamic Analysis of Micelle Formation. The thermodynamic quantities of the micellization for ionic univalent surfactants, the standard free energy ΔG_m, the standard enthalpy ΔH_m, and the standard entropy ΔS_m were calculated through the following relations (x_{CMC} in eq 5 is the CMC in mole fraction unit) and using the above values of CMC and γ, and these values are listed in Table 2:[40]

$$\Delta G_m = (2 - \gamma)RT \ln x_{CMC} \quad (5)$$

$$\left[\frac{\partial(\Delta G_m/T)}{\partial(1/T)}\right] = \Delta H_m \quad (6)$$

$$\Delta S_m = \frac{\Delta H_m - \Delta G_m}{T} \quad (7)$$

Table 2. Thermodynamic Quantities of Micelle Formation Calculated Using Eqs 5−7 for C_6mimBr under Different Temperatures

T (K)	ΔG_m (kJ/mol)	ΔH_m (kJ/mol)	$-T\Delta S_m$ (kJ/mol)
288.2	−18.58	−17.08	−1.49
296.7	−18.63	−14.13	−4.50
313.2	−19.13	−8.93	−10.20
323.2	−19.44	−6.86	−12.58

As listed in Table 2, the values of ΔG_m are all negative. This means micellization of C_6mimBr in aqueous solution is a spontaneous process. In this process, the ΔH_m is associated with the transfer of C_6mimBr monomer from the aqueous environment to the micelle. Before the micellization process of C_6mimBr, the interaction that influences the enthalpy is from mainly a hydrogen bond between C_6mimBr and water molecular. While when the micelle formed, the self-repulsion between head groups and hydrophobic effect of the hydrocarbon chain of C_6mimBr are dominant. The negative ΔH_m indicates that the energy for breaking the hydrogen bond between C_6mimBr and water is lower than that released in micelle formation. This is perhaps because the counterions Br^- reduced the self-repulsion between the head groups and the micellar stabilization was enhanced. In addition, the positive ΔS_m can be considered to be caused by the release of the water molecules frozen around the C_6mimBr hydrophobic tail. Therefore, this micellization process can be regarded as the balance between the transfer of C_6mimBr monomer from the aqueous environment to the micelle and the release of water molecules.[41]

The values of ΔH_m are negative and the values of ΔS_m are positive, suggesting that the micelle formation for C_6mimBr is driven collectively by enthalpy and entropy. The thermodynamic quantities ΔG_m, ΔH_m, and ΔS_m obtained for micelle formation of C_6mimBr are plotted as a function of temperature in Figure 4. ΔH_m increases and $-T\Delta S_m$ decreases with rising

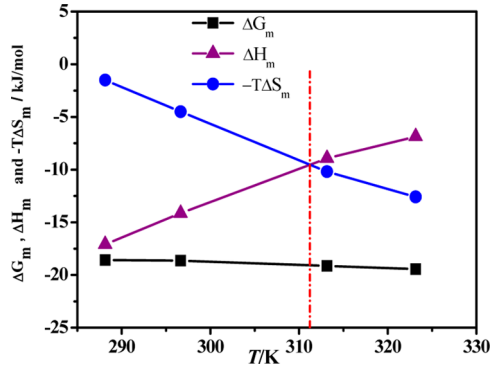

Figure 4. Variation of the thermodynamic quantities of micelle formation with temperature for C_6mimBr.

temperature and at 311 K (crossing temperature), and $-T\Delta S_m$ intersects with ΔH_m. This means that an enthalpy term ΔH_m plays the dominant role to the negative ΔG_m below the crossing temperature, while the contribution from entropy term ΔS_m becomes dominant above the temperature. In other words, the micelle formation process for C_6mimBr is controlled by the enthalpy effect at lower temperature, while it is entropically driven at higher temperature.

3.4. Variance in the Number of Bound Water in the Micellization. *3.4.1. Dielectric Relaxation of Water for the C_6mimBr−Water System.* Figure 5 shows the three-dimensional representations for the concentration dependence of the dielectric spectra (after eliminating the contribution of dc conductivity) for C_6mimBr aqueous solution in the concentration range of 0.4−2.11 M, from which an asymmetric peak of dielectric loss can be observed. The position of the peak has little change with C_6mimBr concentration, located around 10 GHz, and its intensity gradually decreases with the increase of concentration.

For pure water, one relaxation process is needed to describe the complex permittivity at the frequency ranges from 500 MHz to 40 GHz. It is apparent from the asymmetric signal that the addition of C_6mimBr introduces a slower debye relaxation process. In order to examine the dielectric spectra in detail and identify the subrelaxation involved in the main relaxation with asymmetrical distribution, a typical cut at the concentration of

dx.doi.org/10.1021/jp506589f | J. Phys. Chem. B 2014, 118, 13729−13736

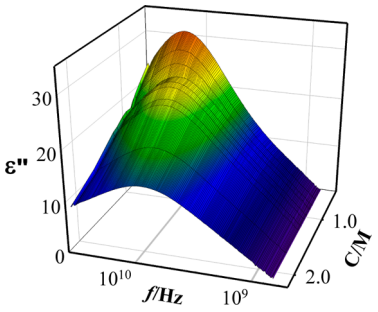

Figure 5. 3D representation for the frequency dependency of dielectric loss spectra after eliminating the effect of the dc conductivity of C_6mimBr solution with different concentrations.

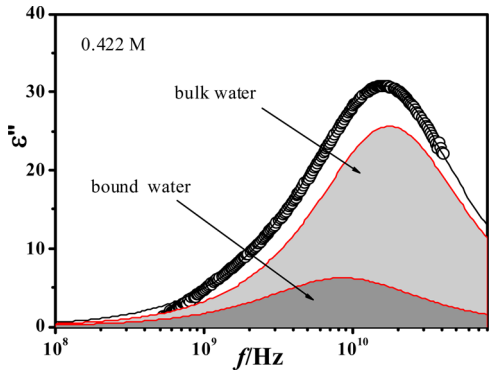

Figure 6. Dielectric loss spectrum of 0.422 M C_6mimBr aqueous solution at 296.7 K. Black open circles represent the dielectric loss after eliminating the effect of dc conductivity, the black line represents the best-fit curve with eq 1, and shaded areas indicate the contributions of the two relaxation modes, respectively.

0.422 M is shown in Figure 6. Strict analysis of the dielectric spectrum was performed according to the method described in section 3.1 and other research.[42] The dielectric loss spectrum was well presented by eq 1 with two Cole−Cole terms (see the black solid line in Figure 6). The fitting result demonstrates that the dielectric spectrum of asymmetrical distribution includes two relaxation processes (or relaxation modes) which were caused by two types of water: the "bulk water" and the "bound water" interacted with C_6mimBr. Similar results were also found for all C_6mimBr concentrations, and the values of the fitting variables are summarized in Table 3. It can be seen that the relaxation time for both bulk water and bound water increases faintly with the increase of C_6mimBr concentration: τ_{bulk} for bulk water increases from 9.36 to 14.47 ps, which is slightly larger than that of pure water (about 9 ps[43]), while τ_{bound} for bound water increases from 19.36 to 27.30 ps in the concentration range of 0.4−2.11 M, which also is consistent with the correlation time from nuclear magnetic relaxation.[44] In addition, the dielectric increment of bound water $\Delta\varepsilon_{bound}$ gradually increases from 15.86 to 22.36 and that of bulk water $\Delta\varepsilon_{bulk}$ gradually decreases from 56.13 to 17.28. All these changes are related to the interactions between water molecules and the head groups and the alkyl tails of C_6mimBr.

3.4.2. Number of Bound Water. Cavell equation[45] is generally used to describe the relation between the dielectric increment $\Delta\varepsilon$ and the effective dipole moment μ of the species responsible for a relaxation process

Table 3. Concentration Dependence of the Dielectric Relaxation Parameters of C_6mimBr Solution at 296.7 K

C (M)	ε_l	ε_m	ε_h	$\Delta\varepsilon_{bound}$	$\Delta\varepsilon_{bulk}$	τ_{bound} (ps)	τ_{bulk}(ps)
0	87.14		12.86		74.28		8.62
0.422	73.83	57.97	1.84	15.86	56.13	19.36	9.36
0.633	72.86	51.02	4.59	21.84	46.43	20.78	11.17
0.760	68.60	45.25	4.21	23.35	41.04	22.22	9.90
0.844	65.60	42.46	3.94	23.14	38.52	23.23	11.35
0.971	65.60	41.09	6.30	24.51	34.79	25.20	11.44
1.055	64.60	40.52	5.26	24.08	35.26	27.28	11.68
1.182	62.03	38.72	6.19	23.31	32.53	26.71	11.78
1.266	61.35	39.47	6.84	21.88	32.63	28.32	11.86
1.688	51.28	31.48	5.01	19.8	26.47	28.46	13.20
2.110	46.85	24.49	7.21	22.36	17.28	27.30	14.47

ε_l, ε_m, and ε_h indicate the permittivity at low, middle, and high frequency, respectively. $\Delta\varepsilon_{bound}$ and $\Delta\varepsilon_{bulk}$ are the dielectric increment for the dielectric relaxation of bound water and bulk water, respectively.

$$\frac{2\varepsilon_l + 1}{\varepsilon_l}\Delta\varepsilon_i = \frac{N_A c_i}{k_B T \varepsilon_0}\mu_i^2 \tag{8}$$

where N_A, k_B, and T are the Avogadro constant, Boltzmann constant, and absolute temperature, respectively, and c_i is the molar concentration of the species i in mixtures. For the pure water, eq 9 is rewritten as follows:

$$\frac{2\varepsilon_l + 1}{\varepsilon_l}\Delta\varepsilon_w^0 = \frac{N_A c_w^0}{k_B T \varepsilon_0}(\mu_w^0)^2 \tag{9}$$

From eqs 8 and 9, we get the following equation from which the concentration of bulk water in C_6mimBr aqueous solution can be calculated

$$c_{bulk} = \frac{\Delta\varepsilon_{bulk}\rho_w^0}{\Delta\varepsilon_w^0 M_w} \tag{10}$$

where ρ_w^0 and M_w are the density and the molar mass of pure water, respectively. The number of bound water per C_6mimBr Z_s can be described as follows

$$Z_s = \frac{c_{bound}}{c} = \left[\frac{(1-w)}{M_w} - \frac{\Delta\varepsilon_{bulk}\rho_w^0}{\Delta\varepsilon_w^0 M_w}\right]\frac{M_2}{w\rho} \tag{11}$$

where M_2 represents the molar mass of C_6mimBr, w is the weight fractions of C_6mimBr, and ρ is the density of C_6mimBr solution. The values of ρ in different concentrations were determined and listed in Table 4, which are in agreement with the results in ref 46. Using eq 11, the number of bound water in different concentrations was calculated, and the results are also summarized in Table 4.

The numbers of bound water in Table 4 are plotted as a function of the concentration of C_6mimBr solution in Figure 7. Interestingly, at the C_6mimBr concentration below the CMC, the number of bound water per free C_6mim^+ cation Z_s^{mon} is about 20 and did not vary with the concentration of C_6mimBr. However, when the C_6mimBr concentration was above the CMC where the C_6mimBr micelle aggregates formed, the number of bound water per C_6mim^+ for the micelle Z_s^{mic} started to decrease gradually until a relatively stable value of about 8−9 was reached, suggesting the stable micelle formed with the release of water molecules. According to the theoretical calculations of the C_6mim^+ cation[47,48] in which

dx.doi.org/10.1021/jp506589f | J. Phys. Chem. B 2014, 118, 13729−13736

Table 4. Density and the Number of Bound Water per C_6mimBr in Different Concentrations at 296.7 K

C (M)	0.422	0.633	0.76	0.844	0.971	1.055	1.182	1.266	1.688	2.11
ρ (g/L)	1013.2	1018.2	1020.6	1023.5	1030.3	1034.6	1036.5	1042. 6	1059. 8	1071.5
Z_s	19.4	19.9	19.9	19.0	17.8	15.3	13.8	12.0	8.6	7.8

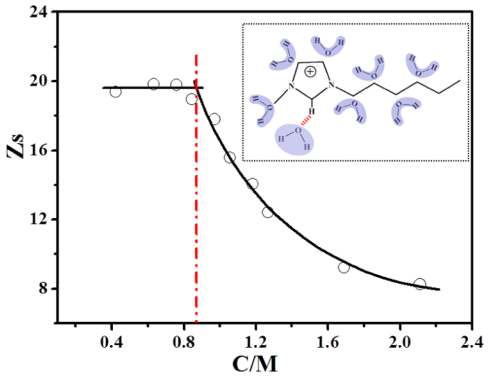

Figure 7. Number of bound water per C_6mimBr calculated from eq 11. The scheme represents the interaction sites of C_6mim^+ and water molecules in the stable micelle.

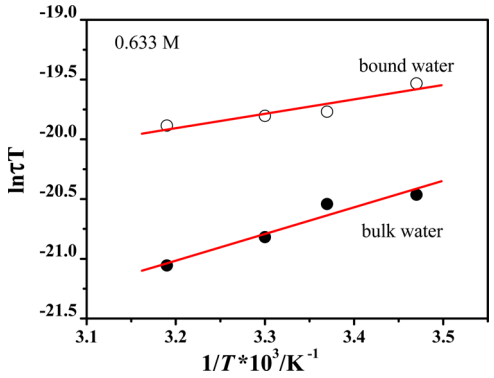

Figure 8. Plots of ln τT against $1/T$ (taking the C_6mimBr concentration = 0.633 M for example). The red solid lines represent the best-fit curves with eq 12.

some acidic sites localized at H-2, H-4, and H-5 of the imidazolium ring and other sites localized at the alkyl chain, water molecules bonded on these about 8 acidic sites and stagnated in micelle inner, as shown in Figure 7. In addition, the result reported by Buchner et al.[49] that the number of bound water per cation in C_8TAB micelle is 9 is also comparable with our result for C_6mimBr.

3.5. Orientation Dynamics of Water in C_6mimBr Solution. It is generally known that the temperature dependence of dielectric spectra can provide thermodynamic quantities for assessing relaxation processes, and then various interactions in C_6mimBr solution can be discussed. The relationship between relaxation time from dielectric measurements and temperature can be determined using the following Eyring equation[50,51]

$$\ln \tau T = \ln\left(\frac{h}{k_B}\right) - \frac{\Delta S}{R} + \frac{\Delta H}{RT} \quad (12)$$

where h is Planck's constant and ΔH and ΔS are the activation enthalpy and activation entropy of relaxation processes, respectively, which are all relevant to the interaction energy between water molecules and C_6mimBr. The ln τT are plotted as a function of $1/T$ for 0.633 M C_6mimBr solution in Figure 8 using the relaxation time data for bulk- and bound-water relaxation processes in Table 3. Obviously, both of the relaxation processes show a good linear relation between ln τT and $1/T$ in the measured temperature range. From the slope and intercept of fitting line, ΔH and ΔS were estimated and are listed in Table 5 together with the data for pure water data taken from ref 43.

As shown in Table 5, the values of ΔH and ΔS of bound and bulk water obtained from the temperature dependence of relaxation time are different from those of pure water: the activation enthalpy of bulk water ΔH_{bulk} is slightly smaller than that of pure water, while that of bound water ΔH_{bound} is much smaller. That is, when the bound water reoriented to the external electric field, it is easier to break the hydrogen bonds of C_6mimBr−water than water−water hydrogen bonds. This implies that the interaction between the electronegative atom

Table 5. Eyring Activation Enthalpy and Activation Entropy of 0.633 M C_6mimBr Solution

C (M)	sample	ΔH (kJ/mol)	ΔS (J·K^{-1}·mol^{-1})
0	pure water	16.09[43]	21.1[43]
0.633	bound water	6.68	−14.62
	bulk water	13.07	10.32

O in water molecule and acidic sites in C_6mim^+ are weaker compared with the hydrogen bond interactions between water molecules. In addition, the dielectric relaxation time for the reorganization of water molecules is directly related to the average number of hydrogen bonds $\bar{n}_{HB}$ that must be broken to obtain "mobile" water molecules, and $\bar{n}_{HB}$ can be calculated by eq 13 using the values of ΔH in Table 5:[31,52]

$$\bar{n}_{HB} = \frac{\Delta H}{\Delta_{HB}H} + 1 \quad (13)$$

Here, $\Delta_{HB}H$ (= 10.9 ± 0.4 kJ·mol^{-1}[53]) is the strength of the H_2O−H_2O hydrogen bonds in the pure water. From this equation, the average number of hydrogen bonds of bulk water $\bar{n}_{HB(bulk-water)}$ was calculated to be 2.2, being close to that of pure water (2.46[54]), and $\bar{n}_{HB(bound-water)}$ is 1.64, being less than that of pure water. This shows that water molecules which were bonded on the C_6mimBr formed smaller clusters (constructral water) with the water molecules around C_6mimBr, causing a physical change in the microenvironment around the C_6mimBr molecules. It is also found from Table 5 that the activation entropy ΔS for both bound water and bulk water are smaller than that of pure water and the thermodynamic quantities for the latter are much closer to that of pure water. It is worth noting that the value of ΔS for bound water is negative; this may suggest that the orientation of hydrogen bond dipoles between water and C_6mim^+ under electrical field resulted in a more ordered cluster structure (see Scheme 2). By contrast, the bulk water molecule reoriented with the adjacent water molecules under external electrical field. This cooperative orientation of bulk water molecules reduced the ordering of the system; as a result, the activation entropy of system goes up.

dx.doi.org/10.1021/jp506589f | J. Phys. Chem. B 2014, 118, 13729−13736

Scheme 2. Orientation of Water Molecules under the External Electric Field[a]

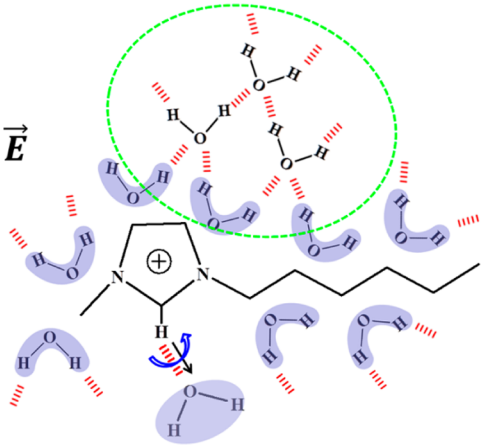

[a]The black arrow represents the dipole of hydrogen bonds between water and C_6mim^+. The blue arrow represents the dipole orientation of bound water. The scheme in the dashed ring shows the ordered cluster structure surrounding the C_6mim^+.

4. CONCLUSIONS

The dielectric relaxation processes of the C_6mimBr−water system were investigated in detail in varying C_6mimBr concentrations and temperatures. The surface activity parameters CMC and γ were obtained by analyzing dc conductivity in different concentrations and temperatures. Further, the thermodynamic quantities of the micellization of C_6mimBr, ΔG_m, ΔH_m, and ΔS_m, were calculated. We found that the mechanism of micellization depends on the temperature: the micelle formation process for C_6mimBr is controlled by enthalpy effect at low temperature, which was decided by the interaction energies of C_6mimBr−water and C_6mimBr−C_6mimBr, i.e., the sum of the contributions from the thermal effect of the bond broken and formed, while the micelle formation process is entropically driven at high temperature, which was decided by the order distribution of component of micelle.

We found that two relaxation processes which originated from orientation polarization of the "bulk water" and "bound water" interacted with C_6mimBr by analyzing the dielectric spectroscopy. We calculated for the first time the number of bound water per C_6mim^+ in the micellar core from the relaxation parameters obtained experimentally and showed that the number of bound water is consistent with the number of acidic sites in C_6mim^+. The essence of cooperative orientation dynamics of water in different environments was described based on the activation enthalpy and activation entropy of relaxation processes: the orientation of bound water resulted in a more ordered cluster structure and the cooperative orientation of bulk water molecules reduced the ordering of system.

In short, this work reports the thermodynamics and various hydrogen-bond interactions of the micellization process of C_6mimBr in water and the structural reorganization of water molecules in this process. Our findings gave a new insight into the micellization of ILs surfactants and their aggregation dynamics and also demonstrated the advantage of dielectric analysis method in evaluating the physical chemistry properties of the dispersion system.

AUTHOR INFORMATION

Corresponding Author

*Phone: +86010-58805856. E-mail: zhaoks@bnu.edu.cn.

Notes

The authors declare no competing financial interest.

ACKNOWLEDGMENTS

We thank Dr. S. Zhao of the School of Geography, Beijing Normal University, for providing the laboratory facilities for high-frequency dielectric measurements. This work was supported by the National Natural Scientific Foundation of China (Grant Nos. 21173025 and 21473012) and the Major Research Plan of NSFC (Grant No. 21233003).

REFERENCES

(1) Greaves, T. L.; Drummond, C. J. Ionic Liquids as Amphiphile Self-Assembly Media. *Chem. Soc. Rev.* **2008**, *37*, 1709−1726.

(2) Greaves, T. L.; Drummond, C. J. Solvent Nanostructure, the Solvophobic Effect and Amphiphile Self-Assembly in Ionic Liquids. *Chem. Soc. Rev.* **2013**, *42*, 1096−1120.

(3) Petkovic, M.; Seddon, K. R.; Rebelo, L. P. N.; Pereira, C. S. Ionic Liquids: A Pathway to Environmental Acceptability. *Chem. Soc. Rev.* **2011**, *40*, 1383−1403.

(4) Blesic, M.; Marques, M. H.; Plechkova, N. V.; Seddon, K. R.; Rebelo, L. P. N.; Lopes, A. Self-Aggregation of Ionic Liquids: Micelle Formation in Aqueous Solution. *Green Chem.* **2007**, *9*, 481−490.

(5) Tariq, M.; Freire, M. G.; Saramago, B.; Coutinho, J. A.; Lopes, J. N. C.; Rebelo, L. P. N. Surface Tension of Ionic Liquids and Ionic Liquid Solutions. *Chem. Soc. Rev.* **2012**, *41*, 829−868.

(6) Chandler, D. Interfaces and the Driving Force of Hydrophobic Assembly. *Nature* **2005**, *437*, 640−647.

(7) Evans, D. F. Self-Organization of Amphiphiles. *Langmuir* **1988**, *4*, 3−12.

(8) Łuczak, J.; Hupka, J.; Thöming, J.; Jungnickel, C. Self-Organization of Imidazolium Ionic Liquids in Aqueous Solution. *Colloids Surf., A* **2008**, *329*, 125−133.

(9) Shi, L.; Zheng, L. Aggregation Behavior of Surface Active Imidazolium Ionic Liquids in Ethylammonium Nitrate: Effect of Alkyl Chain Length, Cations, and Counterions. *J. Phys. Chem. B* **2012**, *116*, 2162−2172.

(10) Zhang, H.; Li, K.; Liang, H.; Wang, J. Spectroscopic Studies of the Aggregation of Imidazolium-Based Ionic Liquids. *Colloids Surf., A* **2008**, *329*, 75−81.

(11) Dong, B.; Li, N.; Zheng, L.; Yu, L.; Inoue, T. Surface Adsorption and Micelle Formation of Surface Active Ionic Liquids in Aqueous Solution. *Langmuir* **2007**, *23*, 4178−4182.

(12) Goodchild, I.; Collier, L.; Millar, S. L.; Prokeš, I.; Lord, J. C.; Butts, C. P.; Bowers, J.; Webster, J. R.; Heenan, R. K. Structural Studies of the Phase, Aggregation and Surface Behaviour of 1-Alkyl-3-Methylimidazolium Halide+ Water Mixtures. *J. Colloid Interface Sci.* **2007**, *307*, 455−468.

(13) Zhao, Y.; Gao, S.; Wang, J.; Tang, J. Aggregation of Ionic Liquids [C N Mim] Br (N= 4, 6, 8, 10, 12) in D2o: A Nmr Study. *J. Phys. Chem.B* **2008**, *112*, 2031−2039.

(14) Smirnova, N.; Safonova, E. Micellization in Solutions of Ionic Liquids. *Colloid J.* **2012**, *74*, 254−265.

(15) Miskolczy, Z.; Sebők-Nagy, K.; Biczók, L.; Göktürk, S. Aggregation and Micelle Formation of Ionic Liquids in Aqueous Solution. *Chem. Phys. Lett.* **2004**, *400*, 296−300.

(16) El Seoud, O. A.; Pires, P. A. R.; Abdel-Moghny, T.; Bastos, E. L. Synthesis and Micellar Properties of Surface-Active Ionic Liquids: 1-Alkyl-3-Methylimidazolium Chlorides. *J. Colloid Interface Sci.* **2007**, *313*, 296−304.

(17) Köddermann, T.; Wertz, C.; Heintz, A.; Ludwig, R. The Association of Water in Ionic Liquids: A Reliable Measure of Polarity. *Angew. Chem., Int. Ed.* **2006**, *45*, 3697−3702.

(18) Jiang, W.; Wang, Y.; Voth, G. A. Molecular Dynamics Simulation of Nanostructural Organization in Ionic Liquid/Water Mixtures. *J. Phys. Chem. B* **2007**, *111*, 4812−4818.
(19) Nandi, N.; Bhattacharyya, K.; Bagchi, B. Dielectric Relaxation and Solvation Dynamics of Water in Complex Chemical and Biological Systems. *Chem. Rev.* **2000**, *100*, 2013−2046.
(20) Gao, Y.; Hilfert, L.; Voigt, A.; Sundmacher, K. Decrease of Droplet Size of the Reverse Microemulsion 1-Butyl-3-Methylimidazolium Tetrafluoroborate/Triton X-100/Cyclohexane by Addition of Water. *J. Phys. Chem. B* **2008**, *112*, 3711−3719.
(21) Graziano, G. Comment on "Water's Structure around Hydrophobic Solutes and the Iceberg Model. *J. Phys. Chem. B* **2014**, *118*, 2598−2599.
(22) Wang, J.; Wang, H.; Zhang, S.; Zhang, H.; Zhao, Y. Conductivities, Volumes, Fluorescence, and Aggregation Behavior of Ionic Liquids [C4mim][Bf4] and [C N Mim] Br (N = 4, 6, 8, 10, 12) in Aqueous Solutions. *J. Phys. Chem. B* **2007**, *111*, 6181−6188.
(23) Dong, B.; Gao, Y. a.; Su, Y.; Zheng, L.; Xu, J.; Inoue, T. Self-Aggregation Behavior of Fluorescent Carbazole-Tailed Imidazolium Ionic Liquids in Aqueous Solutions. *J. Phys. Chem. B* **2009**, *114*, 340−348.
(24) Ao, M.; Kim, D. Aggregation Behavior of Aqueous Solutions of 1-Dodecyl-3-Methylimidazolium Salts with Different Halide Anions. *J. Chem. Eng. Data* **2013**, *58*, 1529−1534.
(25) Vanyúr, R.; Biczók, L.; Miskolczy, Z. Micelle Formation of 1-Alkyl-3-Methylimidazolium Bromide Ionic Liquids in Aqueous Solution. *Colloids Surf., A* **2007**, *299*, 256−261.
(26) Vaghela, N. M.; Sastry, N. V.; Aswal, V. K. Surface Active and Aggregation Behavior of Methylimidazolium-Based Ionic Liquids of Type [C N Mim][X], N= 4, 6, 8 and [X]= Cl−, Br−, and I− in Water. *Colloid Polym. Sci.* **2011**, *289*, 309−322.
(27) Asami, K. Dielectric Properties of Water in Triton X-100 (Nonionic Detergent)−Water Mixtures. *J. Phys.: Condens. Matter* **2007**, *19*, 376102.
(28) Jansson, H.; Bergman, R.; Swenson, J. Relation between Solvent and Protein Dynamics as Studied by Dielectric Spectroscopy. *J. Phys. Chem. B* **2005**, *109*, 24134−24141.
(29) Lima, F. S.; Chaimovich, H.; Cuccovia, I. M.; Buchner, R. Dielectric Relaxation Spectroscopy Shows a Sparingly Hydrated Interface and Low Counterion Mobility in Triflate Micelles. *Langmuir* **2013**, *29*, 10037−10046.
(30) Ono, Y.; Shikata, T. Hydration and Dynamic Behavior of Poly (N-Isopropylacrylamide) S in Aqueous Solution: A Sharp Phase Transition at the Lower Critical Solution Temperature. *J. Am. Chem. Soc.* **2006**, *128*, 10030−10031.
(31) Rahman, H. M.; Hefter, G.; Buchner, R. Hydration of Formate and Acetate Ions by Dielectric Relaxation Spectroscopy. *J. Phys. Chem. B* **2012**, *116*, 314−323.
(32) Asami, K. Characterization of Heterogeneous Systems by Dielectric Spectroscopy. *Prog. Polym. Sci.* **2002**, *27*, 1617−1659.
(33) Mitsumata, T.; Gong, J. P.; Ikeda, K.; Osada, Y. Low-Frequency Dielectric Relaxation of Polyelectrolyte Gels. *J. Phys. Chem. B* **1998**, *102*, 5246−5251.
(34) Carpena, P.; Aguiar, J.; Bernaola-Galvan, P.; Ruiz, C. C. Problems Associated with the Treatment of Conductivity-Concentration Data in Surfactant Solutions: Simulations and Experiments. *Langmuir* **2002**, *18*, 6054−6058.
(35) Tsao, H.-K. Counterion Distribution Enclosed in a Cylinder and a Sphere. *J. Phys. Chem. B* **1998**, *102*, 10243−10247.
(36) Bhattacharya, S.; Haldar, J. Thermodynamics of Micellization of Multiheaded Single-Chain Cationic Surfactants. *Langmuir* **2004**, *20*, 7940−7947.
(37) Ao, M.; Huang, P.; Xu, G.; Yang, X.; Wang, Y. Aggregation and Thermodynamic Properties of Ionic Liquid-Type Gemini Imidazolium Surfactants with Different Spacer Length. *Colloid Polym. Sci.* **2009**, *287*, 395−402.
(38) Gorski, N.; Kalus, J. Temperature Dependence of the Sizes of Tetradecyltrimethylammonium Bromide Micelles in Aqueous Solutions. *Langmuir* **2001**, *17*, 4211−4215.
(39) Škerjanc, J.; Kogej, K.; Cerar, J. Equilibrium and Transport Properties of Alkylpyridinium Bromides. *Langmuir* **1999**, *15*, 5023−5028.
(40) Desnoyers, J. E.; Perron, G. Temperature Dependence of the Free Energy of Micellization from Calorimetric Data. *Langmuir* **1996**, *12*, 4044−4045.
(41) Shimizu, S.; Pires, P. A. R.; El Seoud, O. A. Thermodynamics of Micellization of Benzyl (2-Acylaminoethyl) Dimethylammonium Chloride Surfactants in Aqueous Solutions: A Conductivity and Titration Calorimetry Study. *Langmuir* **2004**, *20*, 9551−9559.
(42) Tielrooij, K.-J.; Hunger, J.; Buchner, R.; Bonn, M.; Bakker, H. J. Influence of Concentration and Temperature on the Dynamics of Water in the Hydrophobic Hydration Shell of Tetramethylurea. *J. Am. Chem. Soc.* **2010**, *132*, 15671−15678.
(43) Buchner, R.; Barthel, J.; Stauber, J. The Dielectric Relaxation of Water between 0 and 35 °C. *Chem. Phys. Lett.* **1999**, *306*, 57−63.
(44) Hernandez, G.; Brittain, H. G.; Tweedle, M. F.; Bryant, R. G. Nuclear Magnetic Relaxation in Aqueous Solutions of the Gadolinium-N-(2-Hydroxyethyl)Ethylenediamine Triacetic Acid Complex. *Inorg. Chem.* **1990**, *29*, 985−988.
(45) Cavell, E.; Knight, P.; Sheikh, M. Dielectric Relaxation in Non Aqueous Solutions. Part 2.—Solutions of Tri (N-Butyl) Ammonium Picrate and Iodide in Polar Solvents. *Trans. Faraday Soc.* **1971**, *67*, 2225−2233.
(46) Shekaari, H.; Mansoori, Y.; Sadeghi, R. Density, Speed of Sound, and Electrical Conductance of Ionic Liquid 1-Hexyl-3-Methyl-Imidazolium Bromide in Water at Different Temperatures. *J. Chem. Thermodyn.* **2008**, *40*, 852−859.
(47) Mele, A.; Tran, C. D.; De Paoli Lacerda, S. H. The Structure of a Room-Temperature Ionic Liquid with and without Trace Amounts of Water: The Role of C-H···O and C-H···F Interactions in 1-N-Butyl-3-Methylimidazolium Tetrafluoroborate. *Angew. Chem.* **2003**, *115*, 4500−4502.
(48) Logotheti, G. E.; Ramos, J.; Economou, I. G. Molecular Modeling of Imidazolium-Based [Tf2n−] Ionic Liquids: Microscopic Structure, Thermodynamic and Dynamic Properties, and Segmental Dynamics. *J. Phys. Chem. B* **2009**, *113*, 7211−7224.
(49) Buchner, R.; Baar, C.; Fernandez, P.; Schrödle, S.; Kunz, W. Dielectric Spectroscopy of Micelle Hydration and Dynamics in Aqueous Ionic Surfactant Solutions. *J. Mol. Liq.* **2005**, *118* (1), 179−187.
(50) Davies, M.; Swain, J. Dielectric Studies of Configurational Changes in Cyclohexane and Thianthrene Structures. *Trans. Faraday Soc.* **1971**, *67*, 1637−1653.
(51) Smith, G.; Shekunov, B. Y.; Shen, J.; Duffy, A. P.; Anwar, J.; Wakerly, M. G.; Chakrabarti, R. Dielectric Analysis of Phosphorylcholine Head Group Mobility in Egg Lecithin Liposomes. *Pharmacol. Res.* **1996**, *13*, 1181−1185.
(52) Buchner, R.; Hölzl, C.; Stauber, J.; Barthel, J. Dielectric Spectroscopy of Ion-Pairing and Hydration in Aqueous Tetra-N-Alkylammonium Halide Solutions. *Phys. Chem. Chem. Phys.* **2002**, *4*, 2169−2179.
(53) Walrafen, G.; Fisher, M.; Hokmabadi, M.; Yang, W. H. Temperature Dependence of the Low-and High-Frequency Raman Scattering from Liquid Water. *J. Chem. Phys.* **1986**, *85*, 6970−6982.
(54) Hawlicka, E.; Dlugoborski, T. Molecular Dynamics Simulations of the Aqueous Solution of Tetramethylammonium Chloride. *Chem. Phys. Lett.* **1997**, *268*, 325−330.